PROPERTIES OF CONFINED PNIPAM-CO-AAC MICROGELS

A Thesis
Presented to
The Academic Faculty

By

Kamil Marczewski

In Partial Fulfillment
of the Requirements for the Degree
Master of Science in the
School of Materials Science and Engineering

Georgia Institute of Technology

May 2011

PROPERTIES OF CONFINED PNIPAM-CO-AAC MICROGELS

Approved by:

Dr. Vladimir V. Tsukruk, Adviser
School of Materials Science and Engineering
Georgia Institute of Technology

Dr. Valeria T. Milam
School of Materials Science and Engineering
Georgia Institute of Technology

Dr. Timothy J. Bunning
School of Materials Science and Engineering
Georgia Institute of Technology

Date Approved: March 28th, 2011

ACKNOWLEDGEMENTS

I would like to thank my adviser, Professor, Vladimir Tsukurk, for the opportunity to conduct research in his facilities and for his advice and support throughout the last two years. I would also like to thank my committee members, Dr. Valeria Milam and Dr. Timothy Bunning.

I would like to express appreciation for the Georgia Institute of Technology and the education that it has provided me through its facilities and professors.

I would like to thank the members of SEMA for their assistance and support, especially Kyle Anderson, who has trained me in the use of several laboratory techniques and provided frequent feedback and advice.

Finally, I would like to express my gratitude to my parents, Mark and Agatha, for their financial and emotional support throughout my college career. Without their continued support, I would not be where I am today.

Funding for this research was provided by AFOSR FA 9550-08-1-0446, FA9550-09-1-0162 and AFRL.

TABLE OF CONTENTS

LIST OF TABLES

LIST OF FIGURES

SUMMARY

Tunable nanostructures have many important uses in thin film applications. Tunability can be achieved by creating a film that has features that respond to external stimuli, such as temperature, humidity, or pH. However, the response can vary greatly between a confined and unconfined case. In the case of confined materials, this response can be greatly reduced, even completely suppressed, which indicates that separate studies must be conducted on confined states in order to better understand their use for real applications.

Microgels have been previously shown to have exceptional responsive properties that depend on their chemical structure and synthesis. Unlike solid thin hydrogel films that respond on the order of hours, microgels arrange on a surface with no external force and create a highly porous layer which responds rapidly, on the order of minutes, to outside stimuli. These properties make microgels a promising candidate for use in tunable thin films. Although the responsive properties of microgels have been extensively studied in solution and unconfined films, this is not indicative of conditions that would most likely have the microgels placed between two stiffer layers of material. Microgels have been shown to respond to glucose concentration, temperature, pH, and light. One well-studied microgel is poly-*N*-isopropylacrylamide copolymerized with Acrylic Acid (pNIPAM-co-AAC). These microgels use the thermal response of pNIPAM combined with the pH sensitivity of pAAC to create a dually-responsive material.

To study the effects of confinement on pNIPAM-co-AAC microgels, we encapsulated these particles within bi-layers of poly(allylamine hydrochloride)-poly(sodium 4-styrenesulfonate) (PAH-PSS) in order to simulate their response within a polyelectrolyte material. Our samples were prepared with a method called tilt-drying, which creates a microgel concentration gradient. This allowed us to study both the confinement caused by the multi-layered film as well as the

effects of microgels on each other. Our results have shown that the change in particle height is unaffected by the concentration of the film, but the thermal response of pNIPAM-co-AAC microgels is significantly suppressed by the encapsulation of microgels into nanoscale layers.

CHAPTER 1: BACKGROUND

1.1 Introduction

Hydrogels are a class of material with exceptional hydrophilic properties, capable of swelling to several times their original size in order to absorb water. Some hydrogels, such as poly-ethylene-glycol (PEG) have been shown to have remarkable biocompatibility, making them useful for various biological applications. This class of polymers has been adapted to a new field in the last twenty years: microgels. Microgels take the properties of hydrogels and apply them to micro-spheres, introducing new physical constraints and mechanics. The increased surface area of these particles accelerates their response to stimuli such as temperature or water, resulting in rapid tunability.

The surface of microgels is highly customizable when combined with various conjugates. Coupled with molecules used for biological targeting and biocompatible materials such as PEG[1], microgels have quickly become another approach in the growing field of controlled drug delivery. Microgels have been applied to several medical applications[2,3] including micro-lenses, thin biocompatible films, and targeted drug delivery. One study has studied microgels sensitive to glucose[4]. These particles are conjugated to respond to low levels of glucose, at which point glucose stored within the microgel can be released from a physical response. This response can serve as an in-situ release of Insulin in diabetic patients over a prolonged period of time, reducing the need for injections, see Figure 1.

Figure 1: Schematic for PNIPAM (core)/P(NIPAM-AAPBA) (shell) Microgel Particles.[4]

Microgel synthesis varies greatly with specific chemical composition, crosslinking density, and solution composition[5-13]. The most common base for microgels today is poly-*N*-isopropylacrylamide (pNIPAM). This hydrogel has been shown to have significant responsive properties when exposed to water and temperature variation. Materials based on pNIPAM have been shown to have a lower critical solvent temperature (LCST) around 32°C[14-17]. Below the LCST, pNIPAM-based materials become hydrophilic and swell with water. Above the LCST, the material undergoes a coil to globule shift, which results in the expulsion of water from the material (a hydrophobic state). This phenomenon has gained pNIPAM microgels the name "smart gels" [18].

Several studies have been performed on the chemical and physical properties of pNIPAM films and microgels[18-33]. One focus of these studies was on the addition of co-polymers to the chemical composition of these gels. Co-polymers have been used to add secondary responsive properties to microgels[34-41]. One example of this is the addition of acrylic acid (AAC). Acrylic acid incorporated into a pNIPAM microgel has resulted in a system that responds to both temperature and pH[42,43]. Under varying pH conditions, microgels with acrylic acid have been shown to swell and de-swell, depending on the buffer solution. At a pH of 3.0, these particles swell rapidly due to the protonation of the AAC groups. At this pH, the thermal response was shown to be unhindered. At a pH of 6.5, the deprotonated microgel loses solvent and becomes less responsive to a thermal shift[6,44]. Alternate modifications to microgels have included the creation of hollow-core microgels and the use of inorganic cores, such as gold. Gold-core microgels have been shown to have optical responsiveness[45]. This method includes multi-layered polymer microgel preparation.

Extensive research has been placed upon the employment of microgels for medical applications[1]. However, the use of their highly tunable response has been limited in the thin film form. The high surface area coupled with a dual responsiveness has the means of creating a new range of tunable materials. Microgels applied in a thin film retain their rapid response[6,44,46,47] and have been shown to arrange hexagonally[48-50], creating a porous layer. Microgels based on pNIPAM have been shown to swell by as much as 200% in fluid. This provides a great range of tunability. Previously, pNIPAM films have been used as a tunable layer in thin films. However, the response of a solid pNIPAM film is slow, on the order of hours[51,52]. This is insufficient for any realistic application. Microgels, on the other hand, are capable of swelling and de-swelling within minutes of the stimulus being applied[44,46,47]. If these properties are extended to a thin film, a dual rapidly responsive thin film can be created.

1.2 Literature Review

Microgels were originally studied in the 1990's, with a steady increase in interest in the 2000's as evidenced by the large increase in citations[,5,14,19,49,50]. Studies have focus dib a variety of aspects ranging from the synthesis methods to characterization and some applications. Microgels have been synthesized with a variety of materials, though pNIPAM is still predominant due its attractive thermal properties. There are many factors involved in the procedure for microgel synthesis, including pH, temperature, and the cross-linker. The cross-linker has a significant impact on the cross-linking density of microgels and their Young's modulus and swelling ratio[47].

In addition to pure polymers, co-polymer microgels have been synthesized to add additional responsive properties. Acrylic acid, for example, has been used to impart a pH[6,44] sensitivity to pNIPAM microgels, giving them a dual response[43]. As seen in Figure 2, another modification

often studied in microgels is the use of a core and core-shell system. Microgels have been synthesized with hollow cores as well as organic and inorganic materials.

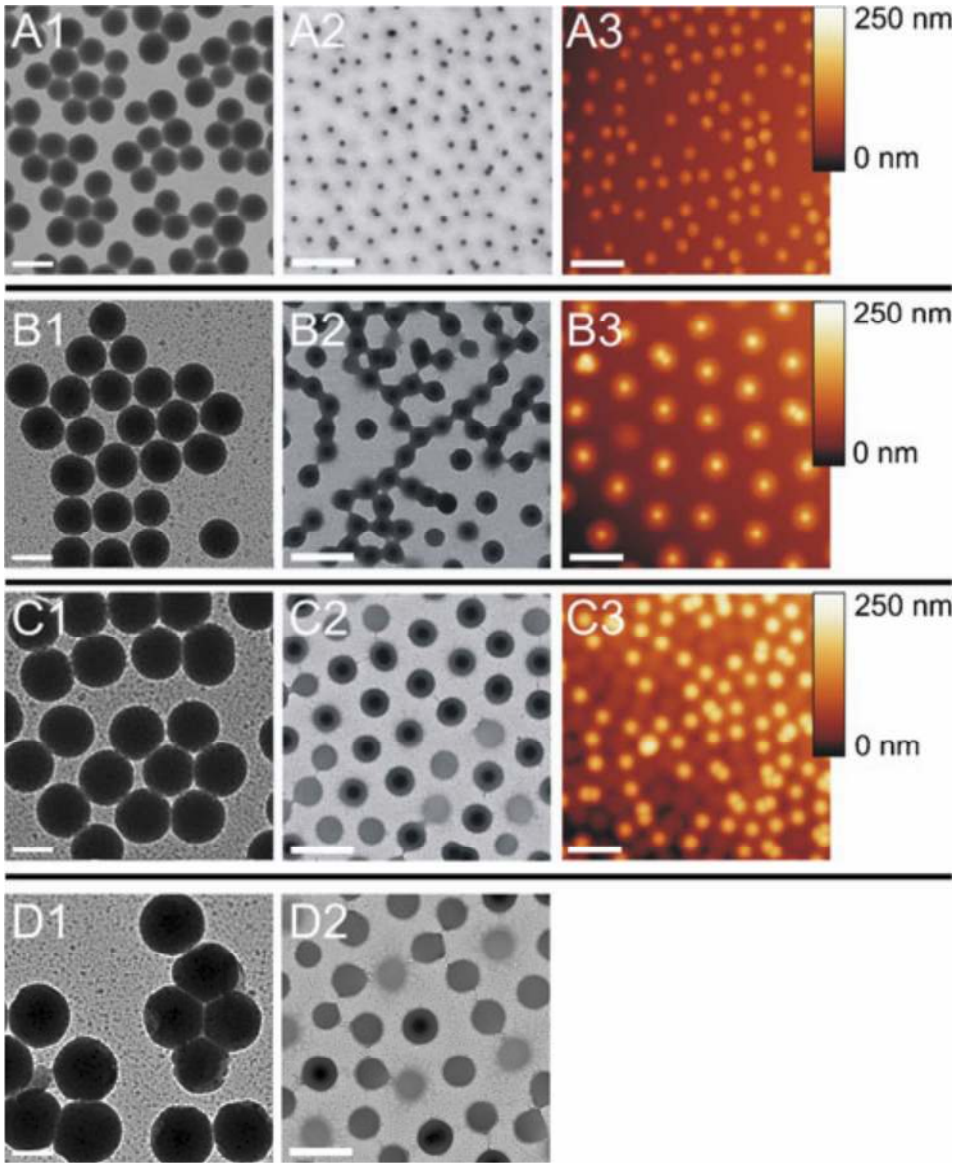

Figure 2: TEM and AFM imaging of Microgel core-shell particles: A1–A3 SiO2-70 and SiO2-70-PNIPAM. B1–B3 SiO2-100 and SiO2-100-PNIPAM. C1–C3 SiO2-140 and SiO2-140-PNIPAM. D1–D2 SiO2-170 and SiO2-170-PNIPAM.[53]

One type of core-shell particle that has been studied is a poly(*N*-isopropylacrylamide) (pNIPAM) (core)/poly(*N*-isopropylacrylamide-co-3-acrylamidophenylboronic acid) (p(NIPAM-AAPBA)) core, which was shown to possess sensitivity to glucose[4]. The goal of this design was to create

a complex particle that could sense glucose levels and release insulin stored within the core when the glucose level reached a certain level. The data showed that the original thermal response was intact while also showing the presence of glucose sensitivity.

Of particular interest was the triple transition that occurred in response to temperature. Due to the complexity of the design, there were essentially three layers to this design. The first was the central core of pNIPAM, which was highly cross-linked; next was a second region of the core, but this one showed a lower cross-linking density; lastly was the heavily conjugated shell. These transitions occurred around the LCST of pNIPAM, but resulted in the same overall response if the particles were heated well above or below the LCST, as seen in Figure 3.

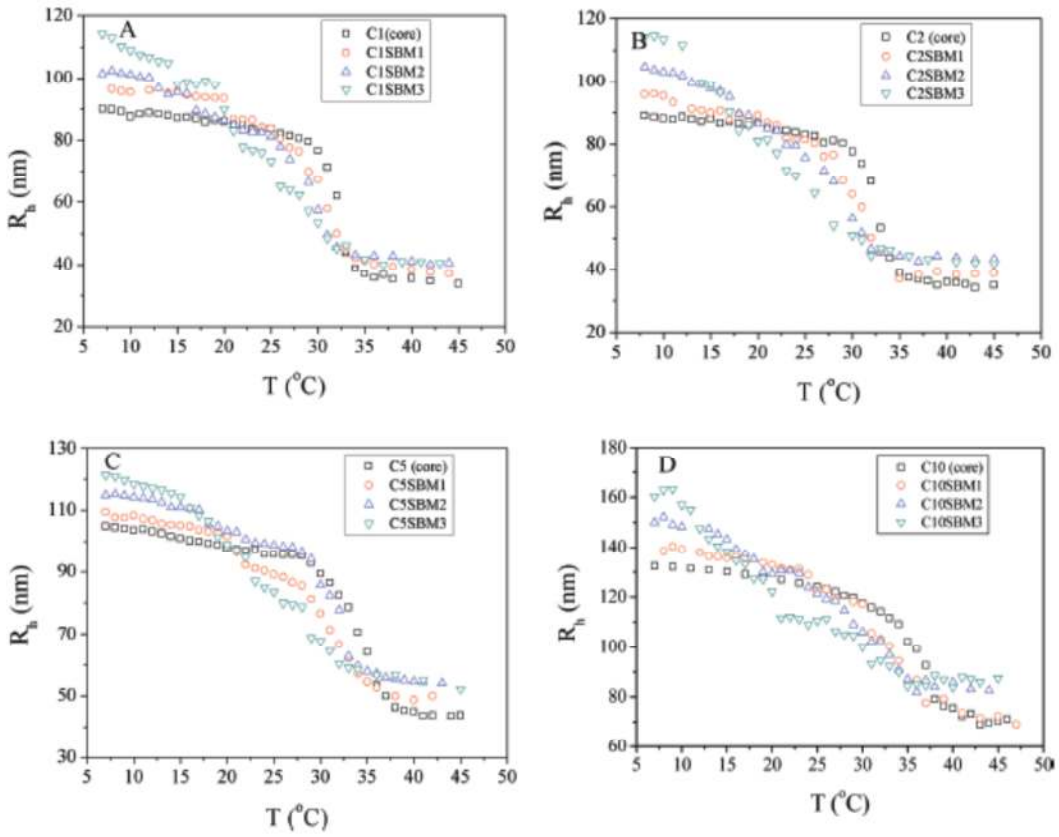

Figure 3: Thermal transition of Glucose-sensitive microgels, showing three definite transitions in microgel thickness[4]

Results for the glucose response were not as high as the authors had anticipated (Figure 4) which, while promising in the direction of self-controlled insulin delivery systems, will probably not be sufficient for medicinal use. In addition to the proposed glucose delivery system, other applications for microgels include bio-sensing, chemical sensing, catalysis, optics, drug delivery, cell-adhesion, pH sensitivity, optical sensitivity, and even magnetic sensitivity.

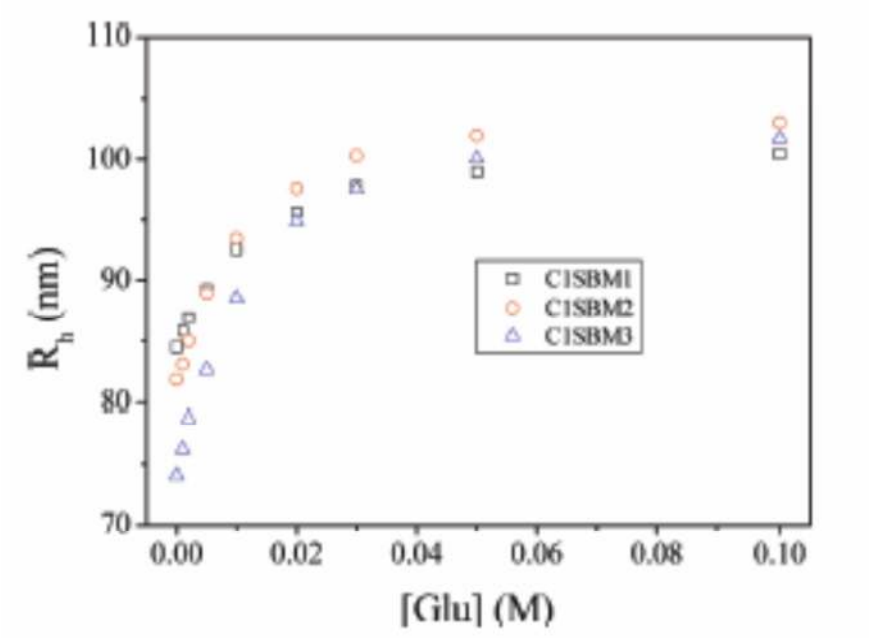

Figure 4: Physical response to glucose concentration[4]

Extensive work with microgels has been performed at the University of Bayreuth, Germany by Schmidt S. et al[54-57]. The first of these works was on the use of microgel films for cell-adhesion. This literature showed supporting evidence for the LCST transition of pNIPAM microgels and the loss of their hydrophilic properties above it. They used this property in order to control cell adhesion to a surface. When below the LCST, the microgels would swell, and release the cells (Figure 5); above the LCST, the microgels would become hydrophobic and thus more prone to attracting the cells to them, via van der Waals interactions and reduced osmotic repulsion. As seen in Figure 5, the cells assumed a spherical shape at 25°C, which was indicative of detachment. After a rinse, most of the cells were removed from the surface, further confirming

that a change occurred in their ability to attach to the surface. Schmidt et al were able to observe this response within 20 minutes of adjusting the temperature and 90% of the cells washed off in a water bath. This supported the rapid thermal response that has been observed in microgels.

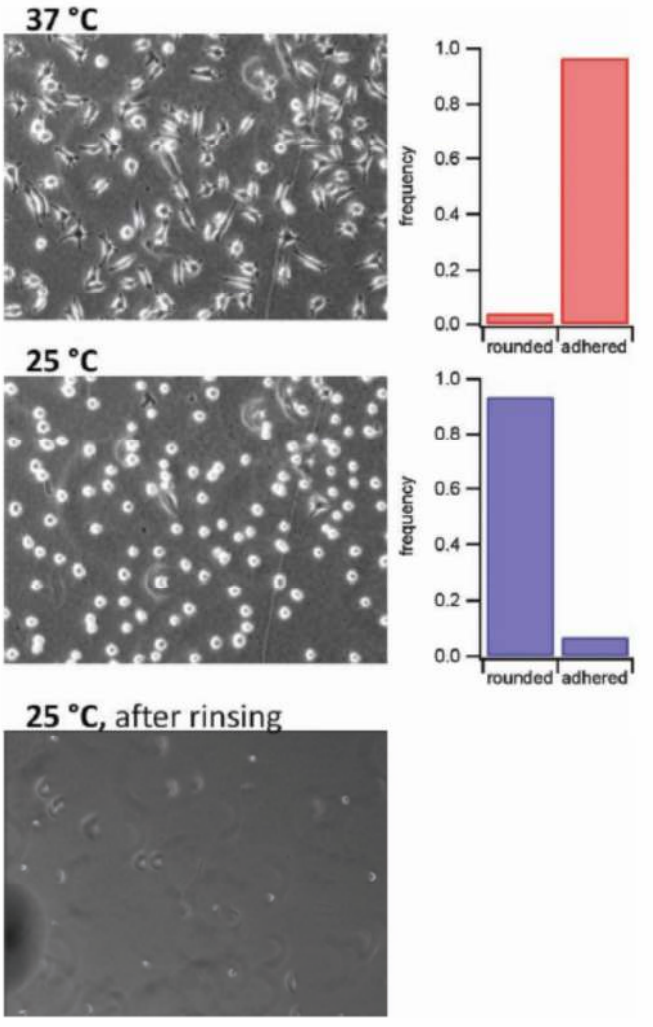

Figure 5: Cell adhesion to microgel layer shift with temperature[57]

The microgels were attached to the surface of the wafer using PEI, which assisted in keeping the microgels from washing away in fluid. This study did not focus on the confinement effects resulting from two layers surrounding the microgel film, nor from the microgels themselves. In addition, this work focused on the use of pure pNIPAM particles, which only have a thermal

response. Atomic force measurements were taken on individual microgels with high precision (Figure 6), but the effects of nearby microgels on each other was ignored. The study has shown a drastic difference in Young's modulus below and above the LCST, in support of previous claims of this response.

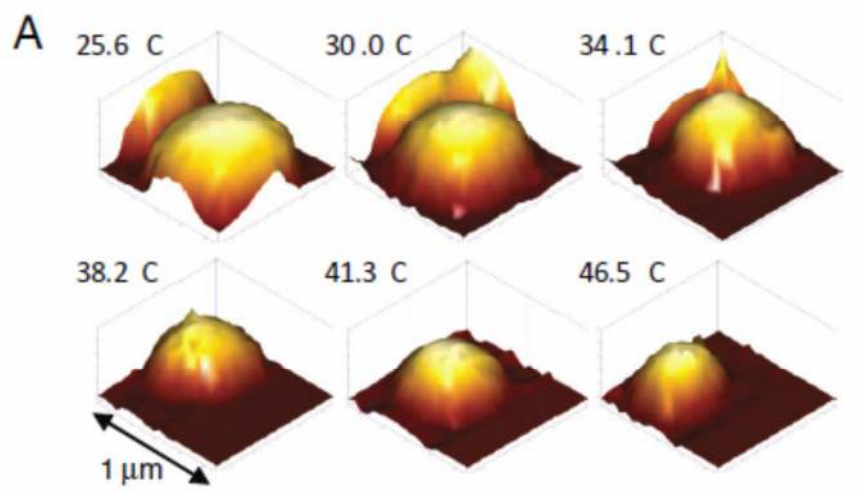

Figure 6: AFM analysis of individual pNIPAm particles with varying temperature[57]

Other work by Schmidt S. et al provided supporting evidence for our work with microgel thin films. Schmidt's et al. goal was to create a simple thermally responsive surface. It was pursued by the use of pNIPAM microgels co-polymerized with acrylic acid similar to the ones studied here. These particles were spin-coated onto a silicon wafer at low speeds (<1000rpm) in order to deposit a uniform layer. Most of this work was conducted with the particles dry, as they were very loosely held onto the surface of the wafer. In fact, this work has concluded that these particles can remain loosely in fluid as long as the pH was kept below 2. Above this pH, over 50% of the particles would lift off. This work focused primarily on the effects of cross-linker density and the resulting films. However, it still provides an excellent reference point for our study.

Ellipsometry data from this work showed a shift in refractive index with temperature. While this shift supported the physical changes seen around the LCST, the refractive index changed by only 0.03, which is not significant for any reasonable optical tunability. The ellipsometry data was used to prove that a thermal response was still present despite the microgels confining each other laterally in a monolayer.

AFM analysis of these particles was conducted in tapping mode using a 42N/m spring constant cantilever. All scans were performed in air, so a thermal response was not investigated using this particular analysis. The purpose of these scans was to determine the difference in microgel morphology with varying cross-linker, as seen in Figure 7.

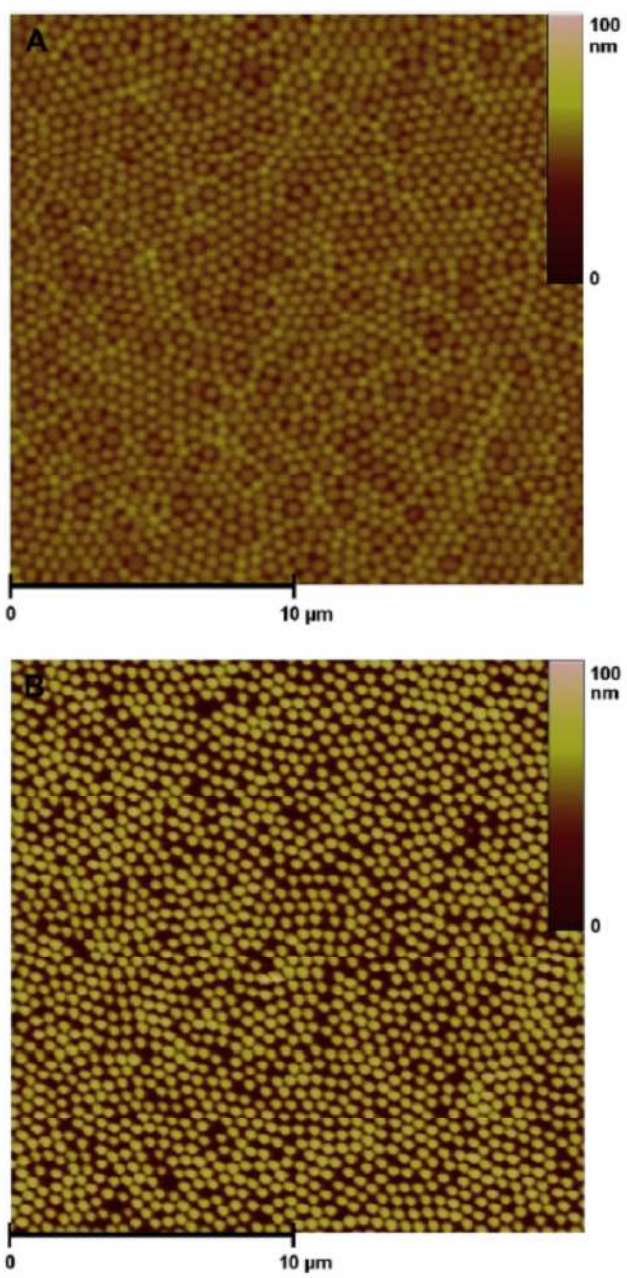

Figure 7: Atomic force microscopy scans of dry microgels. A) 2% cross-linker concentration B) 10%[55]

Diez-Pascual A. and Wong J.[58] have examined the confinement effects on free-floating microgels by using layer-by-layer deposition of polypeptides and polysaccharides. The merit of these films is their versatility in biotechnology, medicine, and drug release. This work focused on the benefits of combining these biopolymers with microgels and the interaction between the

microgel's thermal response and the organization of the layer-by-layer biopolymer. One concern was whether the deposition of these biopolymers would suppress the thermal response of the pNIPAM microgel. To determine this, the authors used dynamic light scattering and electrophoretic measurements. Their results were a collection of thermal experiments with each deposition of biopolymer onto the microgels. Each test proved successful by showing that the thermal response was not suppressed even after several layers are deposited on the microgel (Figure 8).

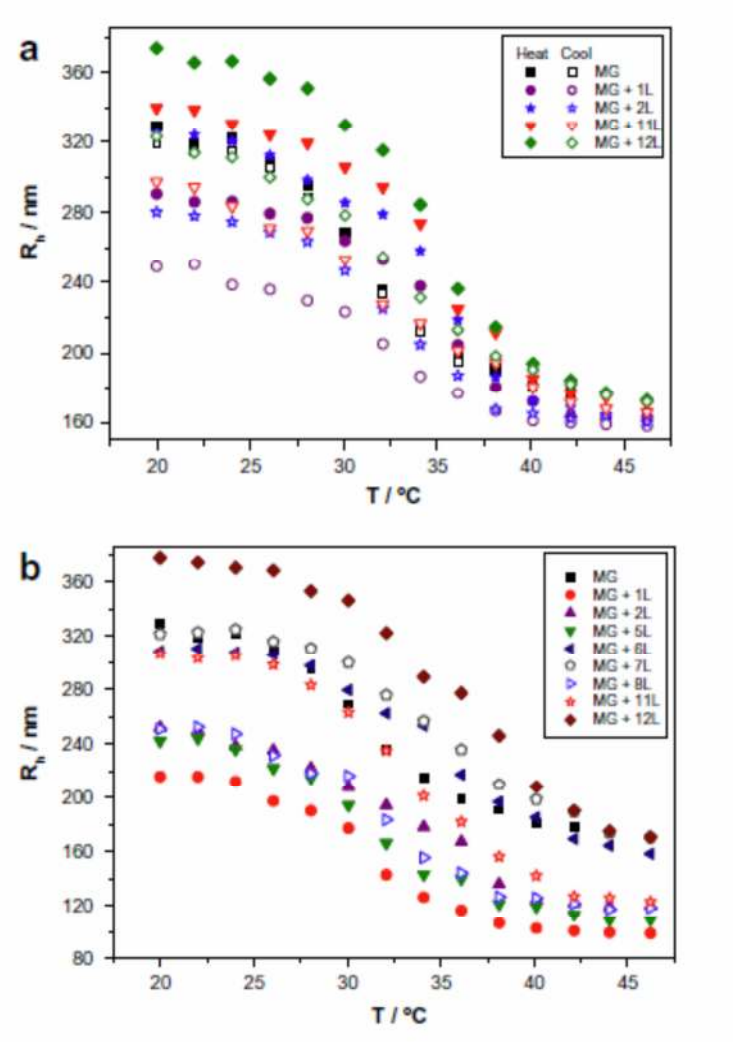

Figure 8: Thermal response of pNIPAM microgels after biopolymer depositions[58]

Of note was the effect of the outermost layer on the radius. Whenever the outermost layer was a polycation, there was a noticeable decrease in the final radius (below the LCST). Whenever a layer of a polyanion was added, an increase in the final radius was observed. This was caused by the electrostatic interaction of the negatively charged microgels and the applied layer. Similar results were observed with the deposition of PSS and PDADMAC multilayers, suggesting that the final layer in a PSS-PAH deposition may have significant impact on the final thickness of the film.

Studies by Serpe[11] and Lyon[11,42] were conducted on the pH-dependency of pNIPAM-co-AAC. In the first study, pNIPAM-co-AAC microgels were tested under varying pH to determine what the effects of the co-polymer and its pH sensitivity had on the thermal response. At a pH of 3.5, results showed that the thermal response followed the typical LCST shift of typical pNIPAM-co-AAC microgels. At a pH of 8.0, the de-protonation of the AAC groups resulted in Columbic repulsion which caused an increase in the de-swelling temperature, normally observed around the LCST. The observed difference of 30°C was significant. These results were followed with the addition of tertbutyl acrylamide (TBAm). TBAm was shown to decrease the phase transition temperature, which was used to tune the transition temperature of microgels to a desired LCST. At a pH of 8, the LCST was reduced by 5°C from the already elevated temperature of 60°C.

The second study conducted by Lyon et al. focused on the pH dependency of microgel thin films. The microgels were deposited on a 2-Mercaptoethylamine (MEA)-functionalized surface and studied under Quarts Crystal Microbalance and Surface Plasmon Resonance for their pH sensitivity. Additional layers of microgels were also deposited by using PAH as a positively charged deposition layer. It was shown that at a low pH of 3.0, the AAC groups and the PAH become fully protonated, which in turn reduced the interaction between the particles and the film, resulting in swelling. On the other hand, at a pH of 6.5, the AAC groups become almost

fully de-protonated, enforcing the interaction between AAC groups and PAH and causing the film to de-swell. The kinetics of the swelling and de-swelling were highly dependent on how many microgel-PAH layers were deposited. Despite the low pH disrupting the AAC-PAH interaction, the film did not dissolve when exposed to those conditions. The authors' theory was that entanglement had occurred between the PAH film and the microgels, but this was outside the scope of the paper. This work provided supporting evidence for our use of pNIPAM-co-AAC microgel films for a pH sensitive tunable thin film. This use of PAH as a supporting layer for multi-layer microgel structures provided insight into the interaction of our microgels with PAH-PSS bi-layers.

CHAPTER 2: OBJECTIVES AND APPROACH

Physical investigations of microgels has been done in solution and when tethered to the surface. It has been shown that biopolymers do not drastically affect the thermal response of microgels; however the outermost layer of biopolymer deposition has significant impact on the particle size and response. However, if microgels are not used as individual particles for medical uses, then they will experience more complicated confined states than have thus far been investigated. If, for example, microgels were used as a responsive layer in thin films, then confinement will be observed from both the neighboring particles as well as the surrounding polymer film. These effects could have a drastic impact on the response of microgels. Further work is required in understanding the confinement effects on microgels. By placing the microgels between two layers of organic or inorganic materials, new previously unobserved constraints may become apparent.

The goal of this study is to investigate the effects of confinement by nanoscale poly(allylamine hydrochloride)-poly(sodium 4-styrenesulfonate) (PAH-PSS) bi-layer films on microgels via atomic force microscopy. PAH and PSS are examples of poly –cations and –anions, respectively. Their Coulumbic interaction with pNIPAM-co-AAC microgels has been previously cited in several studies[11,43], but never in examples of complete confinement. As previous studies into the confinement of microgels for thin films have not been conducted, our work is both novel and useful for the future use of reliable tunable micro-structures.

Samples were prepared with microgels confined within bi-layers of PAH-PSS to determine the effect of polyelectrolyte confinement. The samples were analyzed using atomic force microscopy (AFM) under dry conditions and in fluid. In order to study the thermal response, the temperature was elevated to 45°C, well above the 32°C LCST.

Study Goals:

- Fabricate microgel films with a gradient density
- Determine the confinement effect created on microgels in densely packed thin films.
- Determine the confinement effect of polyelectrolyte layers on the thermal response of microgels

This will involve the following steps:

- Tilt-drying microgels to create a concentration gradient. This allows us to study the confinement created by micro-particles on surrounding particles.
- Layer-by-layer deposition of PAH-PSS bi-layers underneath and over a layer of tilt-dried microgels, creating polyelectrolyte confinement
- Atomic force microscopy investigation of tilt-dried microgels in air and in fluid to study the effects of microgel confinement created in densely packed films
- Atomic force microscopy study of PAH-PSS confined microgels in fluid at room temperature (22ºC) and at elevated temperatures (45ºC) to study the effects of organic confinement on the thermal response.

2.1 Materials selection and Experimental Setup

PNIPAM-co-AAC microgels were provided by researchers at the University of Bayreuth. Studies by light scattering showed that the particles were between 80-100nm in diameter. The concentrated solution of 58.8 mg/ml nanopure water was diluted ten times for thin film deposition. Particles were prepared via aqueous free-radical precipitation polymerization[59,60], resulting in co-polymerized pNIPAM and AAC particles, see Figure 9. To test the organic confinement effect on microgels, bi-layers of poly(allylamine hydrochloride)-poly(sodium 4-

styrenesulfonate) (PAH-PSS) were spin-coated to serve as the polyelectrolyte, see Figure 10. Chemicals were provided by VWR International. PAH and PSS solutions were diluted to 0.2% concentration for spin-coating.

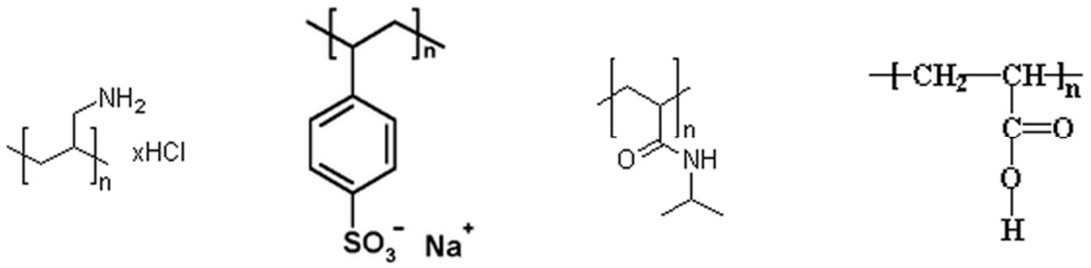

Figure 9: Used polymer chemical structures. From left to right: PAH, PSS, pNIPAM, pAAC

Figure 10: Sample preparation schematic: 1) Spin-coating 2) Microgel Tilt-Drying 3) Second Spin-coating. In the bottom layer, the closest material to the particles is the negatively charged PSS. In the top layer, the closest material is the positively charged PAH.

Polymer films were deposited on atomically flat polished silicon wafers (100), provided by University Wafer, cleaned with piranha solution. Microgels were supplied by Thomas Hellweg, the University of Bayreuth, Germany. The provided microgels were in Nanopure water at a concentration of 58.8 mg/ml.

2.2 Sample Preparation

The microgel solution was diluted ten times for the purpose of sample preparation. Silica wafers were cleaned by piranha solution. Wafers were cut into 1x1 inch squares and sonicated for 30

minutes in 18mΩ Nanopure water. Following the sonic bath, a solution of 90ml hydrogen peroxide and 210ml sulfuric acid was combined to create the piranha solution. The wafers were allowed to sit in the bath for one hour, following five rinses in Nanopure water. Wafers were stored in Nanopure water until used, within two days or less. The resulting wafers had a thin layer of silicon oxide on the surface, made thicker by prolonged exposure to water.

2.2.1 Tilt Drying

In order to test the effects of confinement on both dilute individual particle deposition and on concentrated dense films, microgels were deposited onto the sample surface via a tilt drying method[63]. In tilt drying, the sample was placed at an angle and the microgels are applied via pipette at the top. This allowed the microgel solution to flow down the sample, resulting in a concentration gradient that is dense at the bottom and dilute at the top. The sample was allowed to dry, following further film deposition. The resulting samples ensured that the preparation method used for both the dilute and concentrated case is exactly the same. Tilt drying of microgels was used onto both organic and inorganic films.

Tilt drying was used in order to create a gradient of microgel concentrations on one sample, assuring that the same preparation parameters were used for all data collection, removing human error. The wafer was placed at 45 degrees to the horizontal in a clean petri dish. 100μL of dilute microgel solution was placed drop by drop at the top of the wafer towards the side, giving enough room for a second deposition to be applied, see Figure 11. Excess microgels were collected at the bottom and allowed to drip over the same area three times. This was repeated again on the other side of the wafer, increasing the surface coverage of microgels on the sample. Excess microgel solution was discarded. The microgels were allowed to dry in a fume hood for 30 minutes, with the sample kept at 45 degrees.

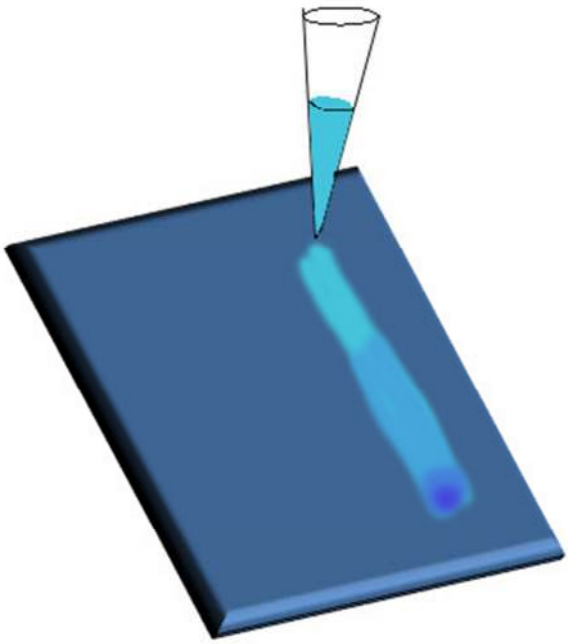

Figure 11: Schematic for Tilt Drying microgel deposition

2.2.2 PAH-PSS Confinement

PAH-PSS bi-layers were deposited onto a silicon oxide wafer via spin-coating. Following three bi-layers of PAH-PSS, microgels were tilt dried onto the surface of the sample, which was followed with another three bi-layers of PAH-PSS spin-coating. Three bi-layers were used in order to assure that the microgels were sufficiently contained within the film.

Standard PAH-PSS solutions were diluted to 0.2% concentration for spin-coating. Samples were spun at 3000 rpm for 30 seconds for all cycles. A cleaned 1x1 inch silicon oxide wafer was used as the base. The first layer deposited was PAH using 300μL of solution. Following the PAH deposition, the wafer was rinsed with a spin-coat of 300μL Nanopure water. Following the rinse, the first layer of PSS was deposited using 300μL of solution, which was followed by another water rinse. This procedure was repeated until three bi-layers of PAH-PSS were deposited onto the wafer. Following this deposition, the sample was prepared for tilt drying.

After the tilt drying step, three more bi-layers of PAH-PSS were spin-coated onto the surface, creating the confinement effect. As each PAH-PSS bi-layer bonded tightly, it can be expected that the PAH-PSS layers above and below the microgels have bonded as well. The resulting film was robust and did not release particles when exposed to fluid.

2.2 Sample Characterization

All AFM images were taken using a Dimension 3000 AFM system. All scans were performed using NSC11-series triangular silicon cantilevers from MikroMesch, with an average spring constant of 3.0N/m, conducted in the light tapping regime[61,62]. A soft cantilever was used instead of a standard cantilever with a spring constant of ~40N/m due to the improved quality of fluid scans that were observed. The images were sharper and particles were more discernible. This is likely due to the soft nature of the microgels where a heavier tapping force would cause drag or clinging on the surface. Initial scans were done in air using a standard cantilever holder.

Subsequent scans were performed in fluid using a specialized fluid cantilever holder. There were two approached to scanning samples in fluid. The first involved gluing the wafer into a petri dish and filling the dish with water. The tip holder was then wetted with a drop and slowly lowered into the dish. Scans like this can easily be done at room temperature, but placing a dish onto a thermal plate adds an additional layer of uncertainty when it comes to vibrational noise in the resulting scan. This method reduces the risk of water evaporating too rapidly during a scan, but that is not a significant concern at room temperature.

The second method involved gluing the sample directly to the thermal plate, see Figure 12. This method required that water be dropped onto the desired scan area as well as on the cantilever holder. The cantilever was lowered into the water drop, similarly to the petri dish. Care had to be taken when lowering the tip as the water distorted the true position of the tip to the surface. It

was often very difficult to focus on the sample surface so it was safer to raise the cantilever higher than normal and lowering it slowly in subsequent scan attempts until the tip and the surface connected. Focusing the tip incorrectly will result in crushing the tip into the surface, requiring the replacement of the cantilever.

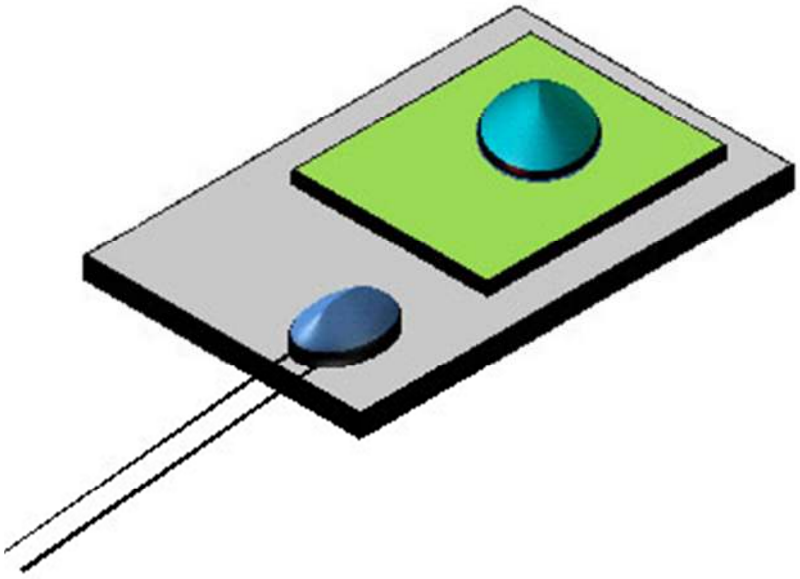

Figure 12: Schematic for thermal fluid AFM analysis (method 2)

In order to scan at elevated temperatures, the second method was employed. For consistency, samples were glued onto a thermal plate with temperature control for all AFM scans. The thermal plate was secured to the AFM base via double-sided tape to reduce vibrations. Scans were performed at 20μm, 10μm, and 5μm at both 22ºC and 45ºC. To bring the sample to 45°C, the temperature was raised gradually and the sample was allowed to sit for 12 minutes. This was sufficient to see the full response induced by going above the LCST. At 45°C, water had to be added to the drop due to excessive evaporation. This was done between scans to reduce vibrations. Following the addition of water, the sample was allowed to sit for 5 minutes to allow the temperature to equilibrate.

CHAPTER 3: RESULTS AND DISCUSSION

In this chapter, the confinement effects on the thermal response of pNIPAM-co-AAC microgels are investigated. Firstly, the tilt-drying method is evaluated and the resulting film is studied under AFM to determine the effects of microgel concentration on their size. This data was collected in air at 22ºC, with the microgels in their collapsed state. Secondly, the effects of PAH-PSS deposition were studied in wet conditions at both 22ºC and 45ºC under AFM.

3.1 Tilt Drying Microgel Deposition

Tilt drying results in a robust concentration gradient (Figures 13 and 14). Depending on the dilution of microgel solution used, the gradient can vary. In the case of the 5mg/ml solution used for these experiments, the visible gradient showed a steep increase in concentration over the length of the sample. In Figures 13A and 14A, particles can be individually measured, with no nearby neighbors. In this case, there was no confinement effect observed on microgels from each other and is used as the control case for the expected microgel size. Figures 13B and 14B, and then 13C and 14C, show a steeply increasing concentration, with more neighboring particles in the B series of images and completely surrounded particles in the C series. In Figure 14C, a distinct hexagonal arrangement can be observed. This organization occurred without any preemptive preparation. This arrangement is not surprising, considering that the greatest possible density of particles can be achieved in hexagonal close packing[64,65]. This results in the lowest favorable energy level for the microgel layer.

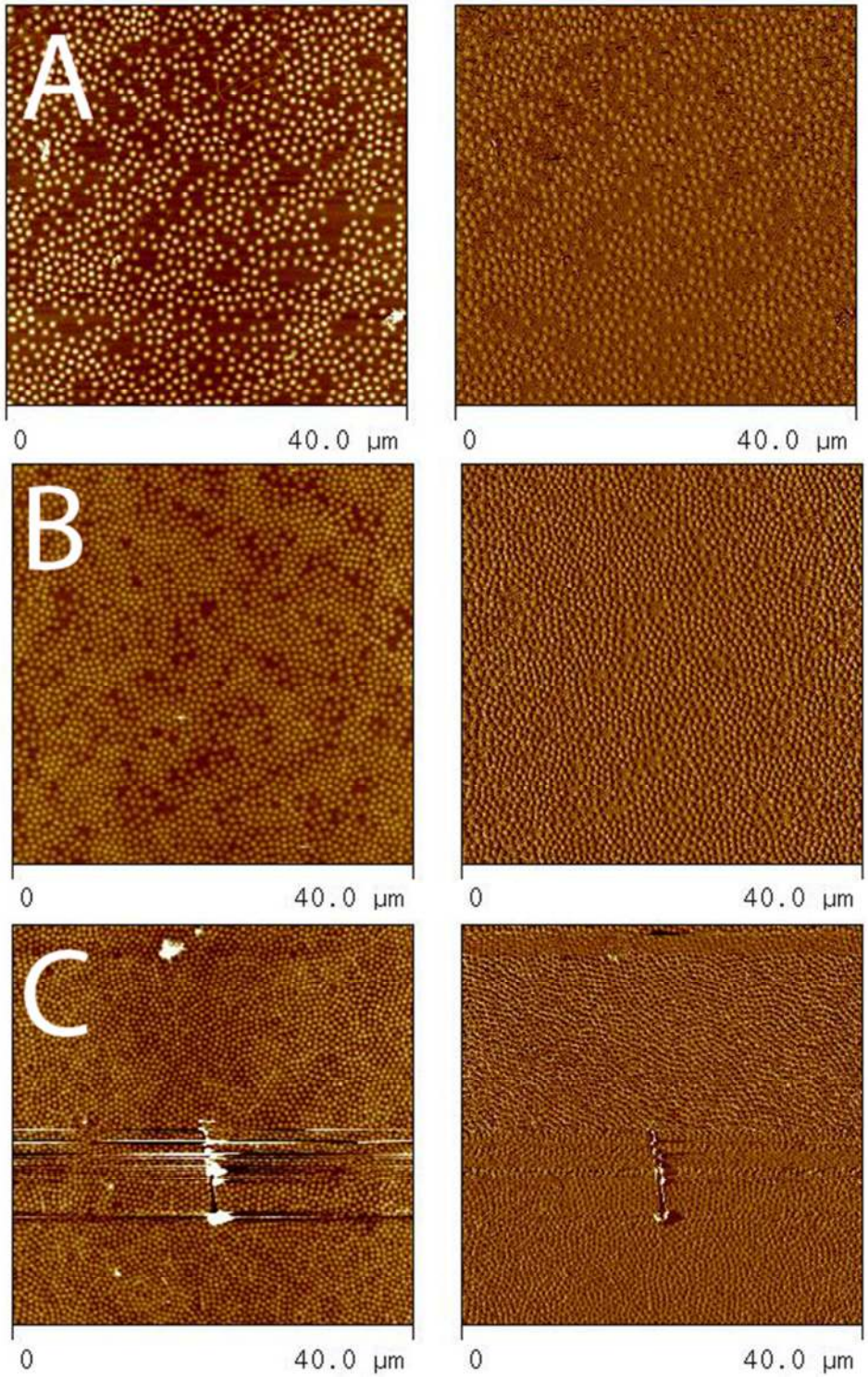

Figure 13: Concentration gradient at 40µm, A-C show low to high concentration in dry state. The first column denotes the height, while the second is the phase. All subsequent AFM images will follow this format. Z = 90 nm

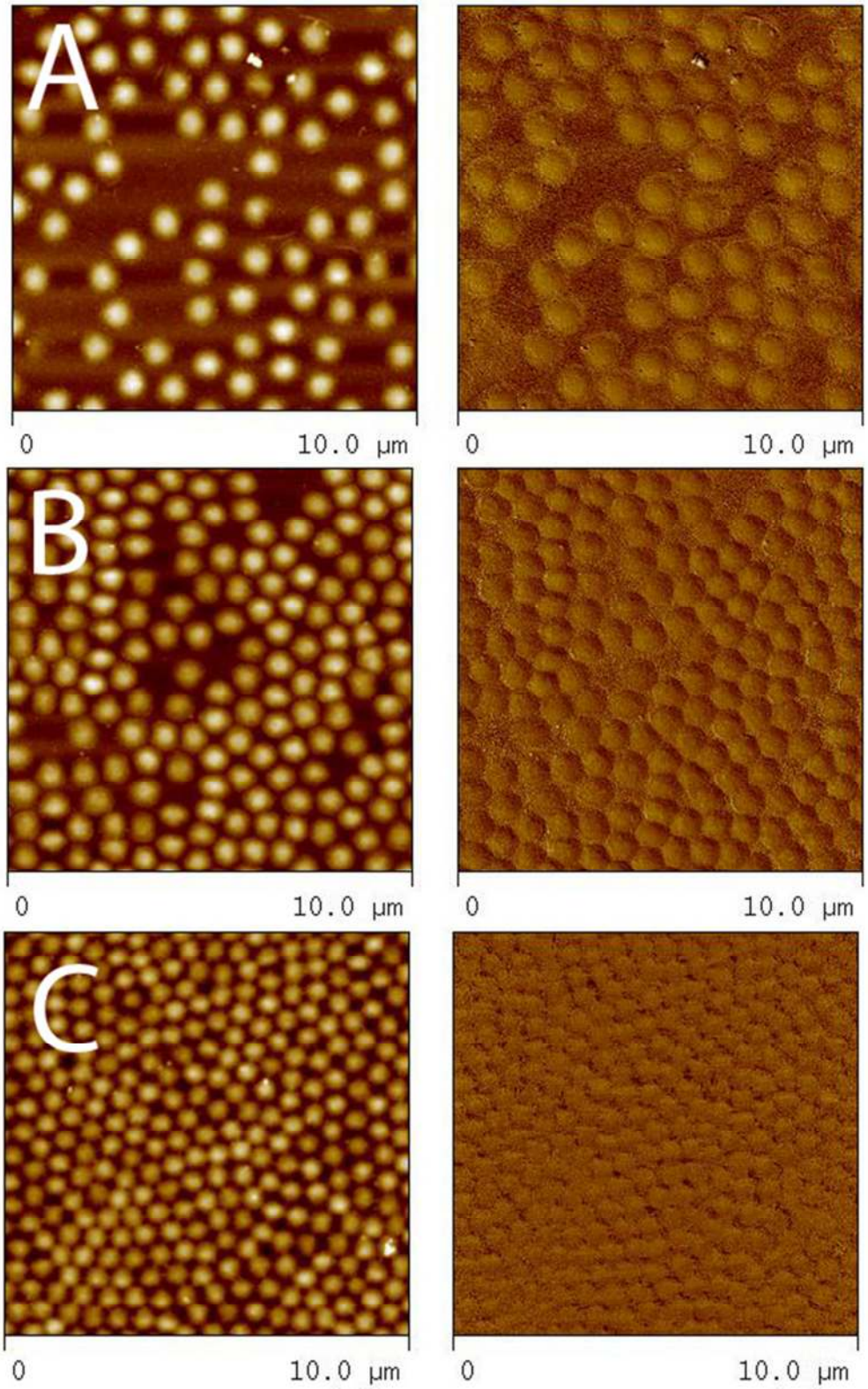

Figure 14: Concentration gradient at 10µm, A-C show low to high concentration in dry state. Z = 90 nm

AFM scans were collected ranging from 40μm to 1μm. The low concentration dry scans, visible in Figure 15, show how individual particles can be effectively studied in this region. All images were manually flattened for height measurements and several cross-sections were taken, as seen in Figures 16-21. In order to accurately measure the height of the particles, all cross-sectioned images were manually flattened using a 1st order of flattening and the particles excluded. This was done to compensate for any curvature that was falsely represented in the height image. As can be seen in the 2μm and 1μm images in Figure 15, there is a thicker deposit clearly visible around each particle. These rings indicate that a thicker than normal deposition of PAH-PSS has occurred around each particle, likely caused by the nature of spin-coating polymer films onto a layer of comparably larger structures (the particles in this case) [66].

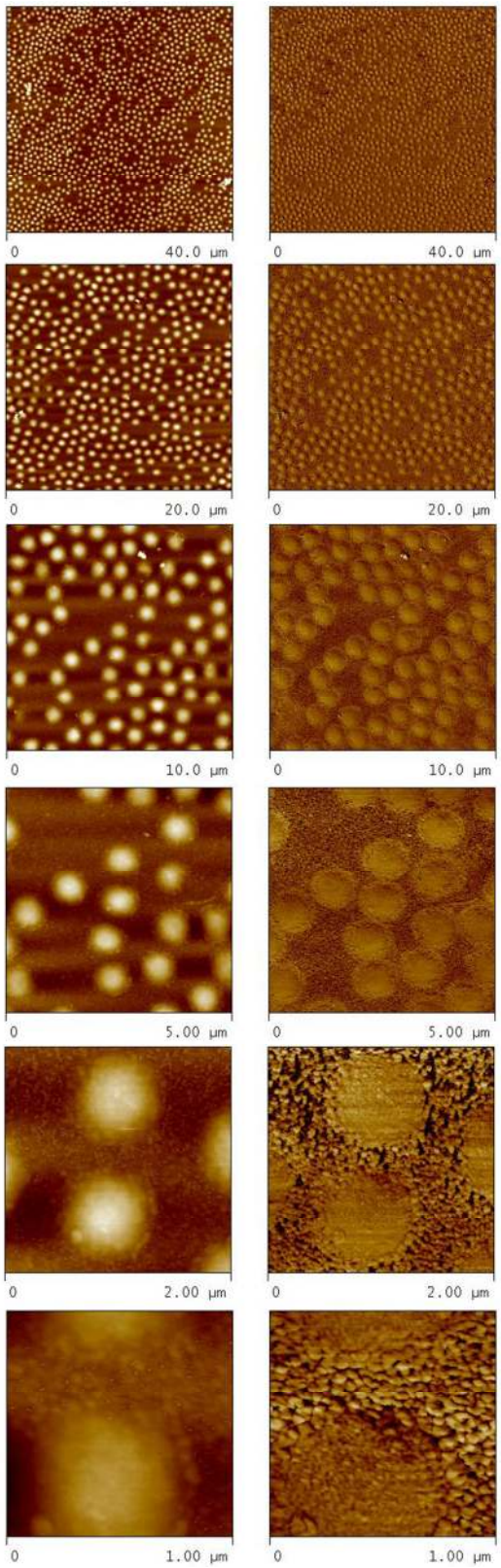

Figure 15: AFM imaging of microgels in air with increasing resolution (low concentration). Z = 90 nm

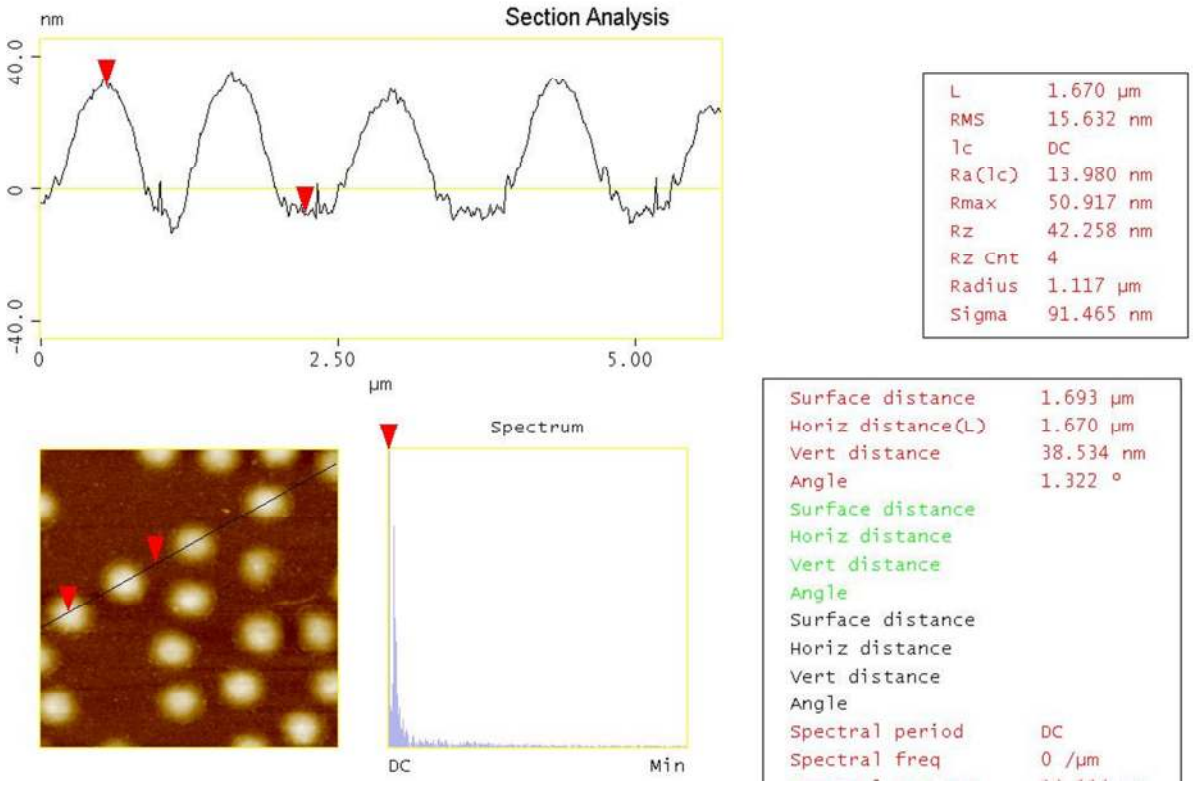

Figure 16: 5µm cross-section scan of dry particles at low concentration

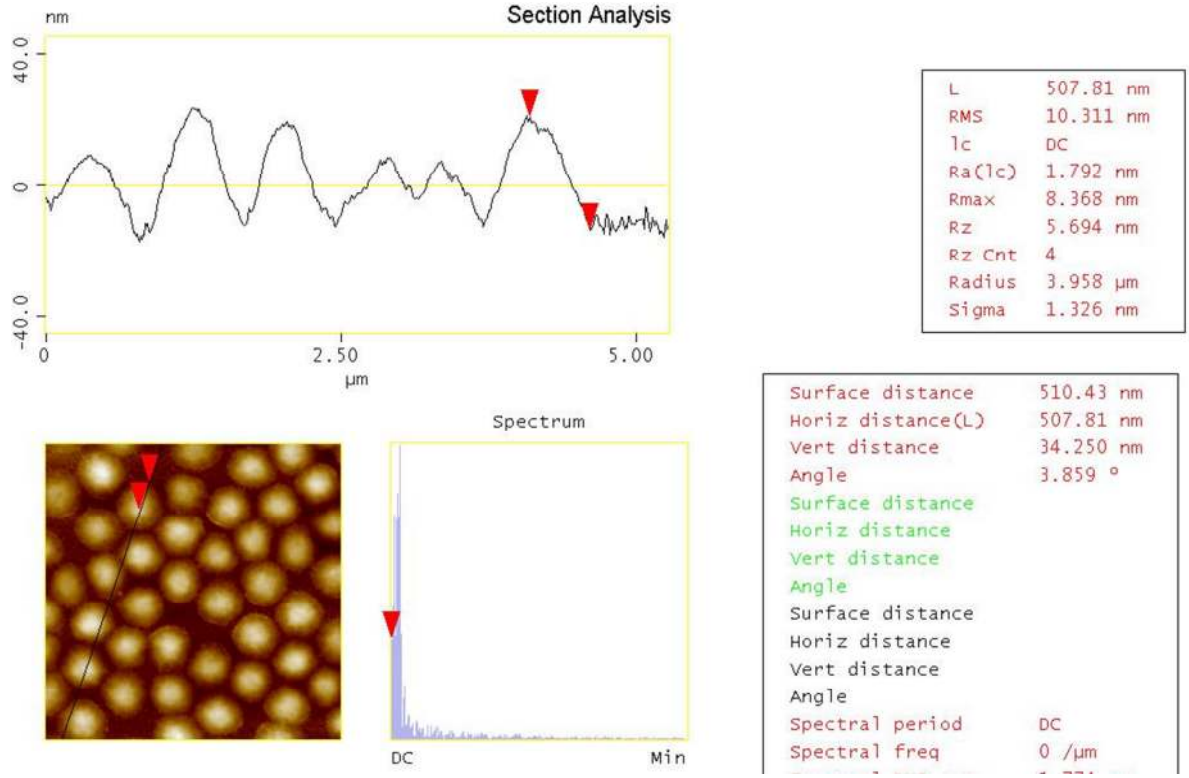

Figure 17: 5µm cross-section scan of dry particles at medium concentration

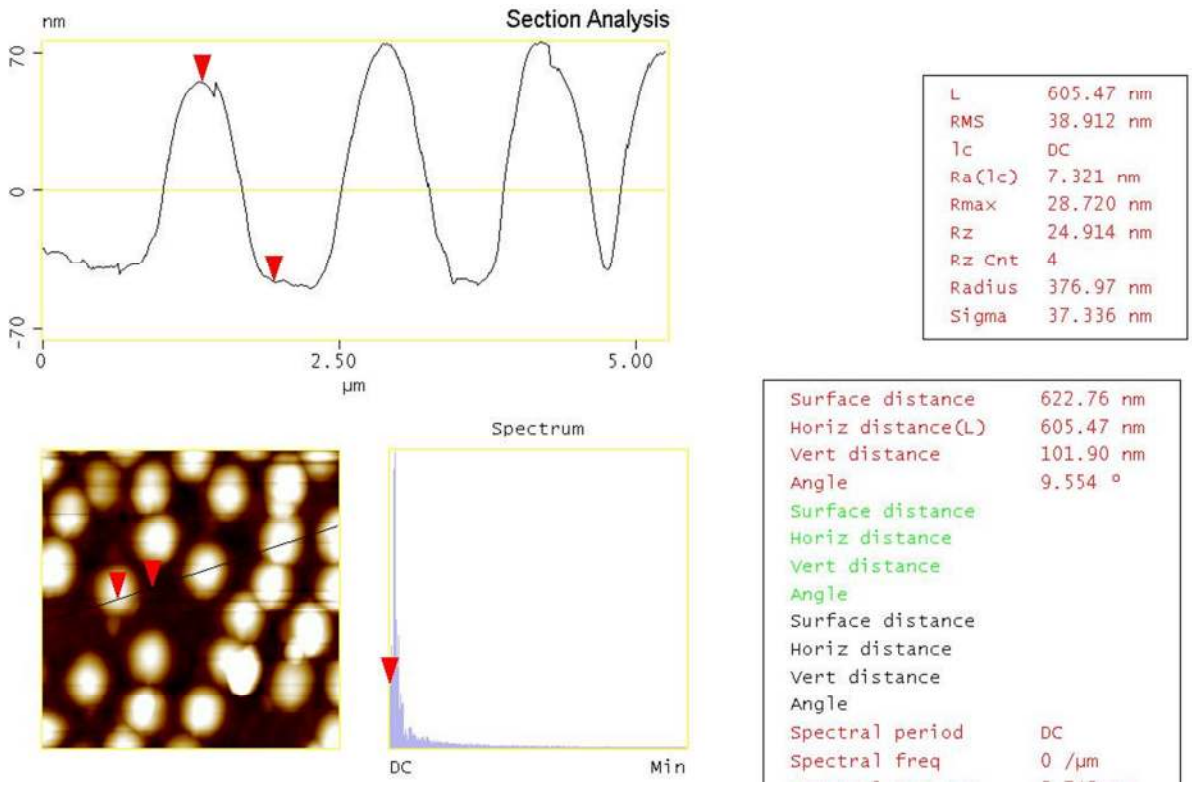

Figure 18: 5µm cross-section scan of wet particles at low concentration (22ºC)

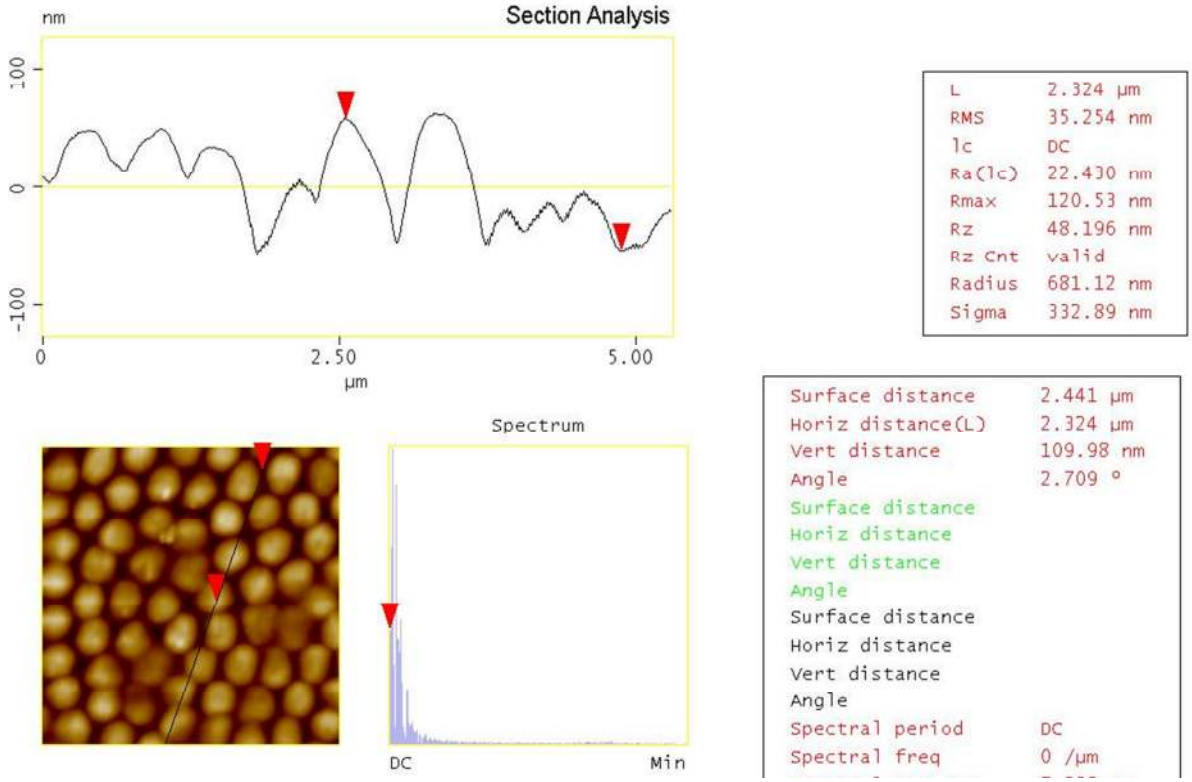

Figure 19: 5µm cross-section scan of wet particles at medium concentration (22ºC)

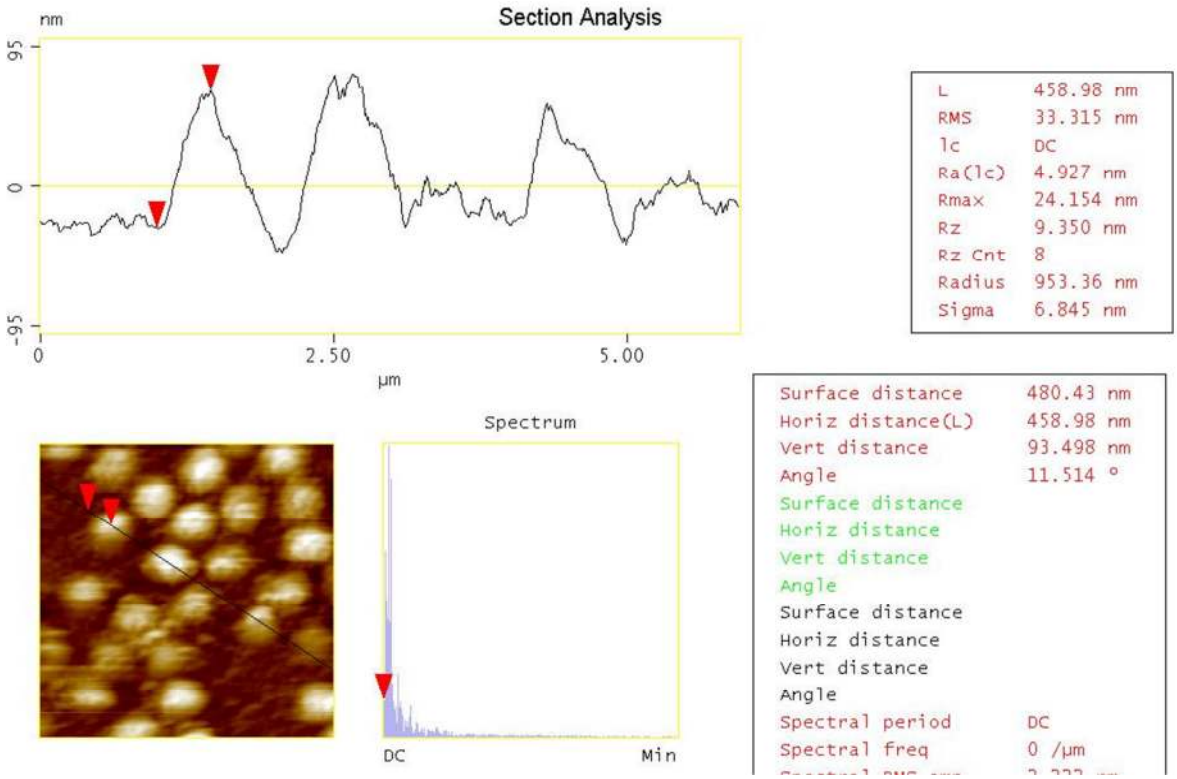

Figure 20: 5µm cross-section scan of wet particles at low concentration (45ºC)

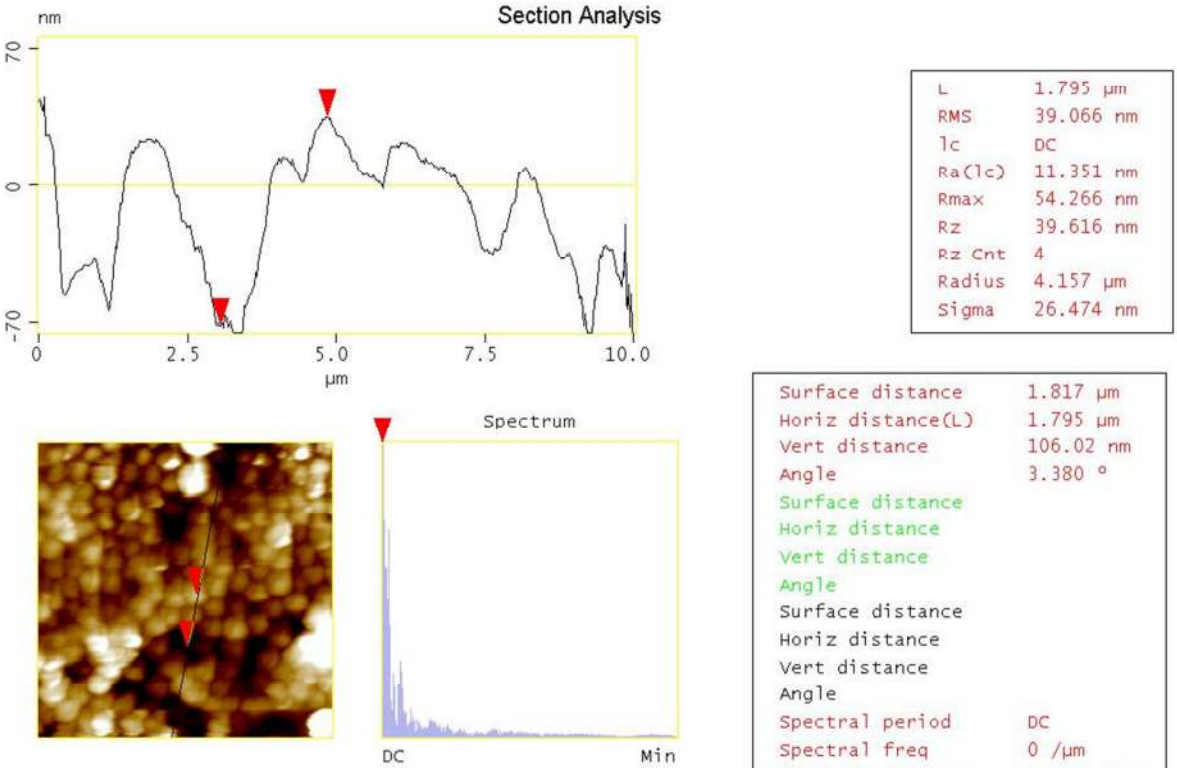

Figure 21: 10µm cross-section scan of wet particles at medium concentration (45ºC)

Based on the cross-sectional height measurements, the average particle height in the dry state was collected at 22ºC, Table 1. There was no evidence that the particle height varied significantly in the three concentration regimes investigated. However, as can be seen in Figure 14, the particles became increasingly compressed in the horizontal plane, suggesting that adjacent particles heavily influenced the particle size when densely packed. However, this compression did not influence vertical expansion.

Table 1: Average height with concentration (dry in air)

Concentration:	Low	Medium	High
Average height (nm):	40 +/-2	39 +/-3	38 +/-2
Difference from unconfined:	100%	97%	95%

For the purpose of a thermal response, this indicated that a concentrated layer of microgels would expand vertically just as effectively as individual particles. To further validate this, we repeated the same scans in fluid at 22ºC and at 45ºC (Tables 2 and 3). In both cases, the microgels showed a statistically insignificant variance in height with particle density.

Based on these results, the tilt-drying method is an excellent approach for studying the confinement of micro-particles in a densely packed layer as it provides consistent preparation parameters with several measurable concentrations on one sample surface. As there was no significant difference in height between low density and high density particles, this study supports the use of a densely packed microgel film as a tunable layer for thin film applications.

Table 2: Average height with concentration (wet at 22ºC)

Concentration:	Low	Medium
Average height (nm):	108 +/-7	107 +/-7
Difference from unconfined:	100%	99%

Table 3: Average height with concentration (wet at 45ºC)

Concentration:	Low	Medium
Average height (nm):	100 +/-3	103 +/-3
Difference from unconfined:	100%	103%

3.2 Confinement Effect of PAH-PSS Deposition

3.2.1 Dry State versus Swollen State

Microgel particles were confined between 2 triple bi-layers of PAH-PSS to study the confinement effect of polyelectrolyte materials on a thin film of microgels. The resulting sample, scanned at resolutions ranging from 40μm to 1μm as seen in Figure 22, shows that only a thin layer of PAH-PSS was deposited as the microgels could be easily distinguished from the surrounding surface. The PAH-PSS was still sufficient for holding the particles in place. The microgels did not wash away in fluid after repeated wetting and drying cycles. A typical scan session involved rewetting the sample several times at room temperature, and rewetting at each resolution at elevated temperatures due to evaporation. This was in contrast to other work[55], where simply spin-coating microgels onto a surface had pH restrictions or other conditions necessary to keeping the particles attached to the surface.

When placed in water, the microgels and the surrounding PAH-PSS deposition swelled. Both the microgels and the organic film absorbed water readily. However, since the films were so thin, their change in thickness was small in comparison to the microgel layer and was disregarded for the purpose of this study. To determine the ability of the microgels to swell regardless of confinement, the sample surface was covered with drops of water in the scanned area. The resulting film swelled by 50% from the dry state (see Table 1 and 2). Since the swelling caused by PAH-PSS alone was insufficient to cause such a large change in thickness, this showed that PAH-PSS films did not prevent water from reaching the microgels. Swelling

occurred nearly instantaneously and no time was required between water application and sample analysis. The surface of the sample, where microgels were present, appeared cloudy, but could not be observed on the AFM screen when in fluid. When the water was removed, but before the microgels were allowed to de-swell, there was a profound deep-blue iridescent pattern visible. This image disappeared as the microgels released water over the next thirty minutes. While the microgels absorbed water readily and swelled, releasing the water at room temperature took time. For this reason, fluid scans were never done before dry scans without a prolonged waiting period.

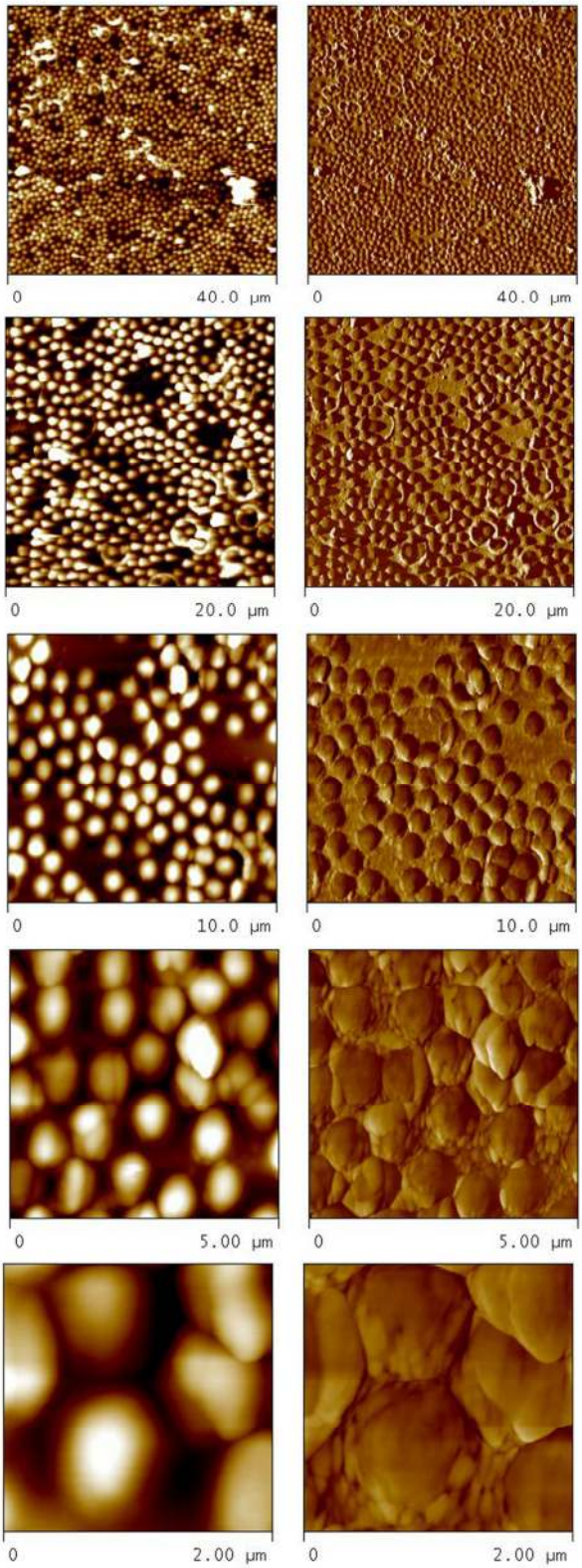

Figure 22: AFM imaging of microgels in fluid with increasing resolution at 22 ºC (low concentration). Z = 150 nm

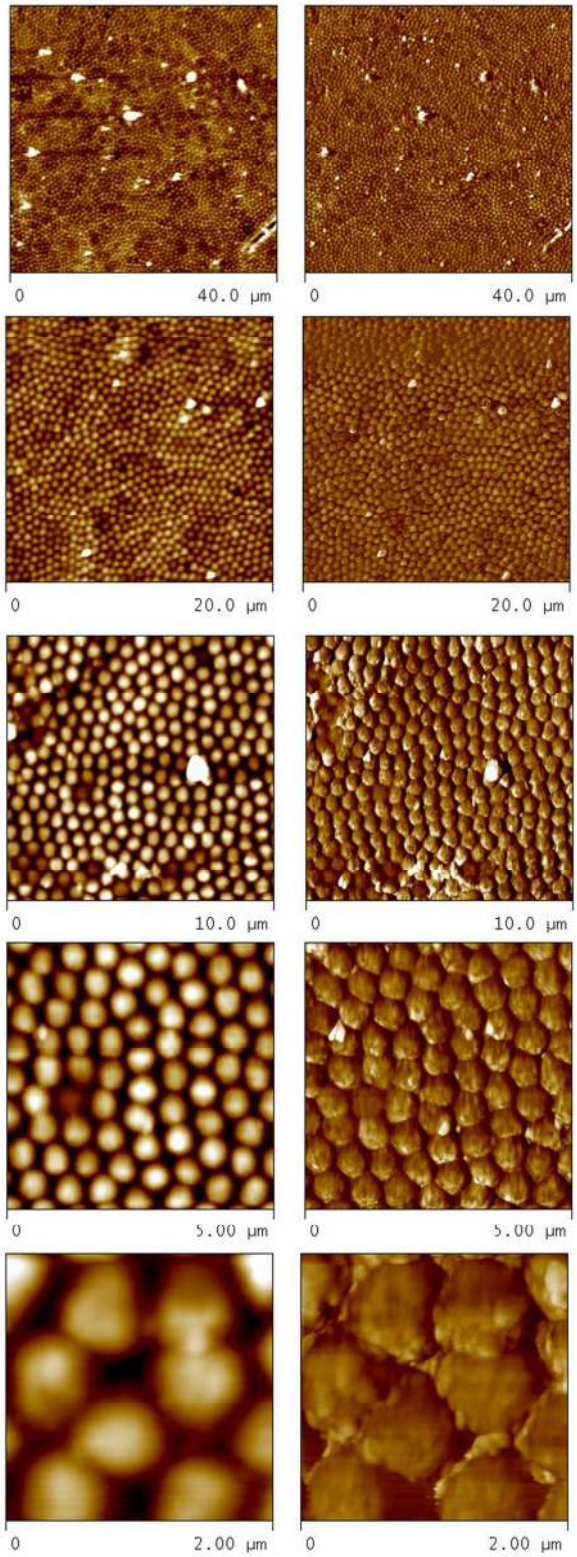

Figure 23: AFM imaging of microgels in fluid with increasing resolution at 22 ºC (medium concentration). Z = 150 nm

3.2.2 Room Temperature versus Elevated Temperature

Microgels experience an LCST shift above 35ºC. At 45ºC, previous literature[55-57] has shown that most physical changes to the microgels have occurred by this point. To determine whether a thermal response still exists in our samples, additional AFM scans were performed at 45ºC. Based on fluid AFM imaging at 45ºC, Figures 24 and 25, we collected height data at a temperature that should be well above the LCST. As can be seen at the smaller resolutions, it became increasingly difficult to collect sharp images due to the increased temperature and fluid mechanics that already dampen the signal strength. In addition, the elevated temperature weakened the adhesive keeping the sample on the thermal plate, which may have increased vibrations in the scan. Based on our results, cited in Tables 2 and 3, we have observed a significantly suppressed response. Table 4 shows the comparison between room temperature and elevated temperature. The observed difference was only 6%. Based on previous result, microgels were expected to change in size by as much as 50%[39]. The referenced study was conducted on similar microgels, but in free-floating solution. As such, it serves as a reference point for an extreme case. Though we expected there to be a reduced response due to the presence of the poly-electrolyte layers, the complete suppression of the response, as observed here, is unusual.

Table 4: Average height with temperature

Average height (nm):	22ºC	45ºC
Low Concentration	108 +/-7	100 +/-3
Medium Concentration	107 +/-7	103 +/-3
Difference from RT	100%	94%

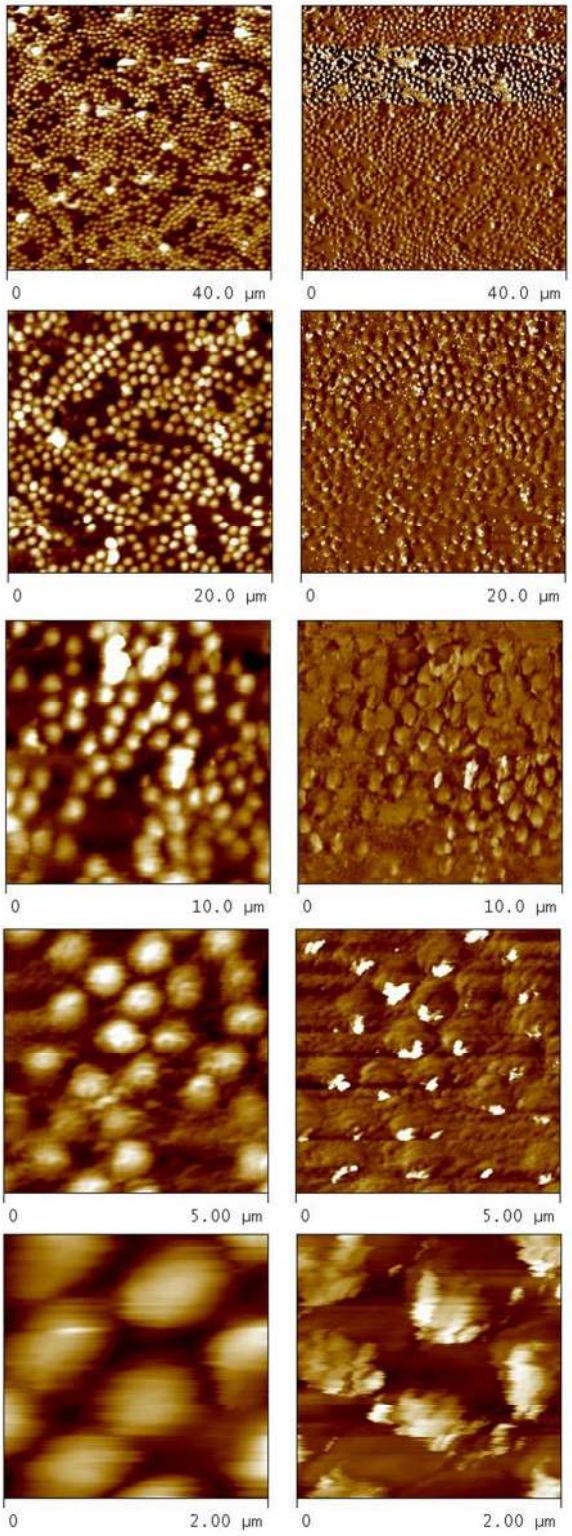

Figure 24: AFM imaging of microgels in fluid with increasing resolution at 45ºC (low concentration). Z = 150 nm

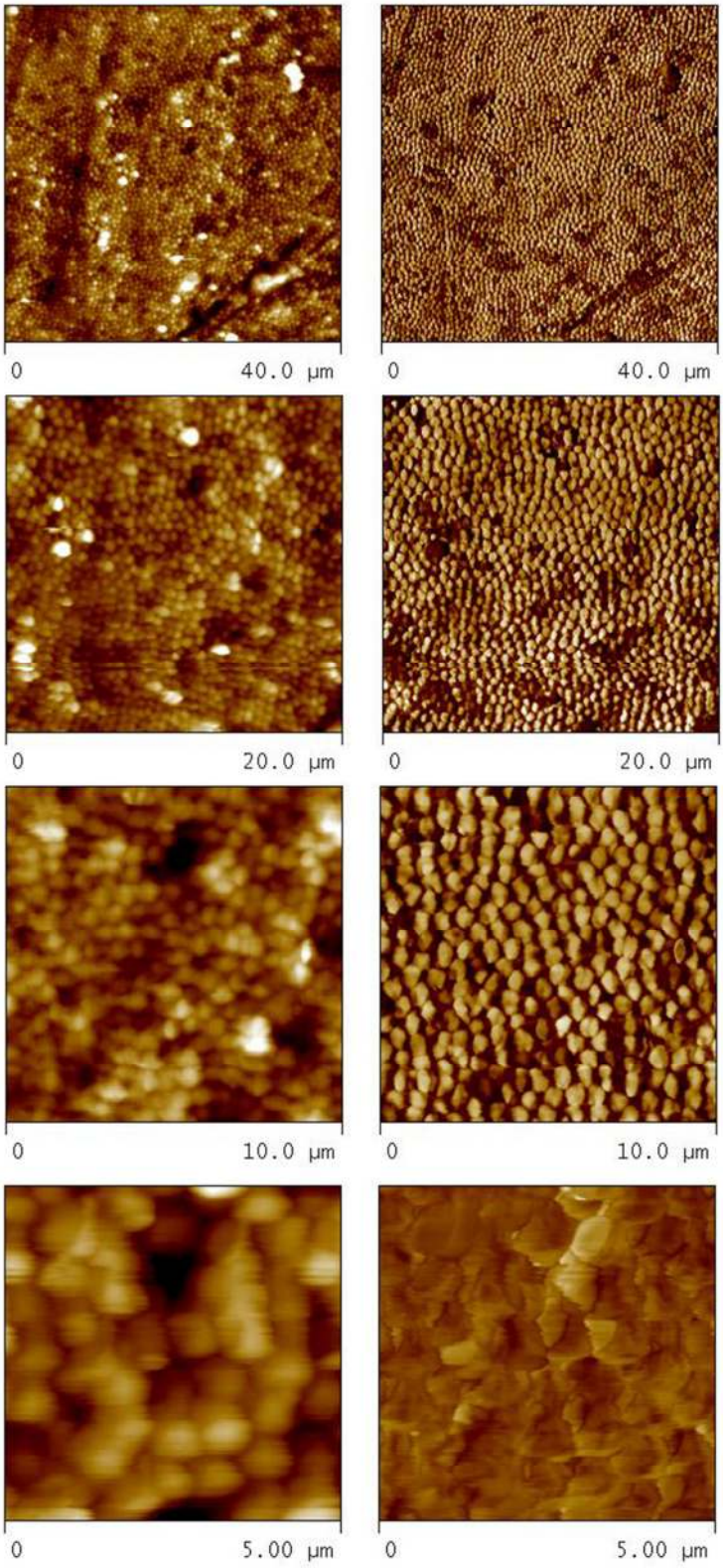

Figure 25: AFM imaging of microgels in fluid with increasing resolution at 45ºC (medium concentration). Z = 150 nm

Previous results[35,39,55-57] have shown a significant shift in particle size when the temperature was elevated. One study[6] showed a change from 170 nm to 60 nm, a 65% change. Based on our results, there was no significant change around the LCST, indicating that confining pNIPAm-co-AAC microgels between PAH-PSS bi-layers did not serve as a proper model for confined response. Since the microgels were kept at an elevated temperature for prolonged periods of time, time was not a factor. We ruled out the possibility that there was a discrepancy between the measured temperature and the temperature at the sample. Several temperature measurements in fluid at the microgel surface revealed that there was only a 1ºC difference in the extreme case.

Previous work[42] has shown that the LCST of microgels can be significantly shifted. In that case, the study was performed using pH variation, see Figure 26. The LCST was shown to have been shifted by as much as 15ºC. However, this study was not conducted on the effects of charged organic layers, but on large variations in pH. It is possible that a similar phenomenon has occurred here, which will require further investigation.

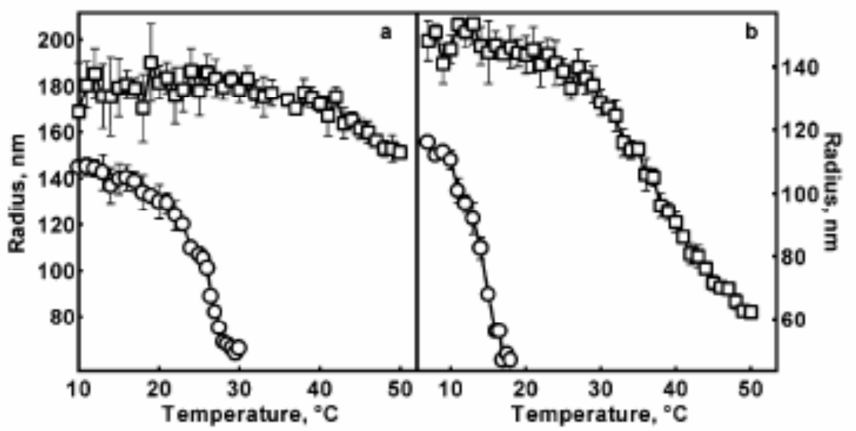

Figure 26: LCST shift with pH, circles = pH 3.5, squares = pH 8.0[42]

Work by Serpe et.al.[11,43,67] has shown that there was a significant interaction between pNIPAM-co-AAC microgels and PAH layers. This response was particularly strong around a pH of 6.5,

when the AAC groups in the microgels become fully charged. PAH has been observed to be fully ionized at neutral pH[68]. In this state, the PAH charges overcompensate for the negative charge of the PSS, which results in a net positive charge in the polyelectrolyte layers. Coupled with the inherently negative charge of the pNIPAM-co-AAC microgels[43], the resulting interaction can cause a reduced response, see Figure 27. We would also like to draw attention to the deposits discussed earlier in Figure 14. These deposits of PAH-PSS surrounding the particles increase the number of layers effectively interacting with each microgel

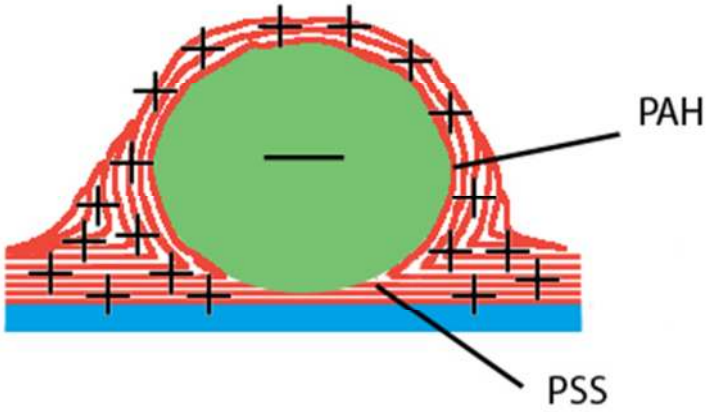

Figure 27: Coulumbic interaction between PAH layer and microgels

Since these experiments were only conducted with three bi-layers of PAH-PSS per spin-coated section, we cannot conclude that fewer polyelectrolyte bi-layers would have shown a smaller dampening effect. However, as evidenced by previous work[68], when the outermost adhesion layer interacting with pNIPAM-co-AAC microgels is PAH, an increased particle surface coverage was observed. In the case of our model, the first layer of the top polyelectrolyte bi-layers was PAH. This suggests that a large fraction of the particle's surface area is exposed to the positively charged PAH layer, which would have occurred in our study regardless of how many bi-layers were deposited. An alternative to studying less bi-layers would be to expose the

microgels to PSS as the starting layer. The negative charge of the PSS should promote the de-swelling of the microgels above the LCST, but would likely reduce the swelling behavior observed below the LCST. Also, as the PAH-PSS model has proved to be unsustainable for a thermal response in microgels, other polyelectrolytes should be selected to determine whether microgels are an applicable option for tunability in such an environment.

CHAPTER 4: CONCLUSIONS

4.1 Experimental Conclusions

In this work, we studied the following:

- Tilt-drying of microgels onto a substrate, the resulting concentration gradient, and the effects of concentration on microgel morphology.
- The effects of two-sided confinement on pNIPAM-co-AAC microgel particles by polyelectrolyte deposition.

Results showed that tilt-drying is a viable method for particle confinement analysis. Using one sample with consistent preparation parameters, several microgel concentrations were investigated. With increased concentration, the amount of nearby particles for each microgel was increased, which also increased the amount of horizontal confinement observed, as seen in Figure 14. However, there was no change in height with concentration, suggesting that microgel on microgel confinement was only relevant in the horizontal. This was supported further with the analysis of microgels in fluid at 22ºC and 45ºC.

The typical thermal response observed in microgels around the LCST was found to be completely suppressed when the microgels are confined within PAH-PSS bi-layers. The previously observed thermal response of 65%[6] height change was reduced to 6%. The change in height was measured to be less than 10 nm, which is insufficient for any practical tunable thin film. For this reason PAH-PSS confinement is not an ideal model for determining whether microgels can serve as a tunable layer in organic thin films. As other materials were not investigated, the use of microgels for such a purpose cannot be ruled out and warrants further investigation.

4.2 Future Work

To continue the study of microgels for tunable thin films, several studies should be undertaken:

- In order to re-affirm the results cited here, an ellipsometry study should be conducted on the polyelectrolyte-confined pNIPAM-co-AAC microgels.
- As PAH has been previously shown to have a strong interaction with microgel particles, the use of fewer bi-layers may have an impact on the significant suppression of the thermal response observed here and should be investigated.
- The use of an uncharged material may yield a better thermal response in the pNIPAM-co-AAC microgels when under confinement.
- As the pH response of the pNIPAM-co-AAC microgels was not investigated under double polyelectrolyte confinement, it is possible that the pH response of these particles would be more significant than the thermal response.
- A proper investigation of the Young's modulus of these films should be conducted using AFM to provide more supporting evidence for the conclusions presented here.

REFERENCES

1 Kessel, S., Schmidt, S., Muller, R., Wischerhoff, E., Laschewsky, A., Lutz, J., Uhlig, K., Lankenau, A., Duschl, C., Fery, A. *Langmuir* **26**, 3462–3467 (2010).

2 Tanaka, T. *Phys. Rev. Let.* **40**, 820-823 (1978).

3 Shibayama, M., Tanaka, T. & Han, C. *J. Chem. Phys.* **97**, 6829-6841 (1992).

4 Luo, Q. *App. Mater. and Int.* **2**, 760-767 (2010).

5 Dagallier, C., Dietsch, H., Schurtenberger, P. Scheffold, F. *Soft Matter* **6**, 2174-2177 (2010).

6 Jones, C. & Lyon, A. *Macromolecules* **33**, 8301-8306 (2000).

7 Kuckling, D., Vo, C., Adler, H., H.-J. P., Voelkel, A., Coelfen, H. *Macromolecules* **39**, 1585-1591 (2006).

8 Oh, J. *Prog. Poly. Sci.* **33**, 448-457 (2008).

9 Pelton, R. *Adv. Col. Int. Sci.* **85**, 1-33 (2010).

10 Scherzinger, C., Lindner, P., Keerl, M., Richtering, W. *Macromolecules* **43**, 6829-6833 (2010).

11 Serpe, M., Jones, C. & Lyon, A. *Langmuir* **19**, 8759-8764 (2003).

12 Wu, K. & Lai, S. *Colloids and Surfaces B: Biointerfaces* **56**, 290-295 (2007).

13 Zhang, J. *J. Am. Chem. Soc.* **126**, 7908-7914 (2004).

14 Murray, M. *Adv. Col. Int. Sci.* **54**, 73-91 (1995).

15 Pelton, R. *J. Col. Int. Sci.* **85**, 1-33 (2000).

16 Nayak, S. & Lyon, A. *Angew. Chem., Int. Ed.* **44**, 7686-7708 (2005).

17 Ballauff, M. & Lu, Y. *Polymer* **48**, 1815-1823 (2007).

18 Ghugare, S., Chiessi, E., Telling, M., Deriu, A., Gerelli, Y., Wuttke, J., Paradossi, G. *J. Phys. Chem. B* **114**, 10285-10293 (2010).

19 Hashmi, S. & Dufresne, E. *Soft Matter* **5**, 3682-3688 (2009).

20 Hendrickson, G. *Adv. Func. Mater.* **20**, 1697-1712 (2009).

21 Hu, X., Tong, Z., Lyon, A. *J. Am. Chem. Soc.* **132**, 11470-11472 (2010).

22 Aslam, K. *Col. Int. Sci.* **312**, 697-704 (2007).

23 Borras, A., Sanchez-Valencia, J., Garrido-Molinero, J., Barranco, A., Gonzalez-Elipe, A. *Microporous and Mesoporous Materials* **118**, 314-324 (2009).

24 Borras, A. & Gonzalez-Elipe, A. *Langmuir* **26**, 15875-15882 (2010).

25 Chia-Lung, L. *J. Pol. Sci. A* **44**, 356-370 (2005).

26 Crowther, H., Morris, G., Vincent, B., Wright, N. *NATO Sci. Ser. IV* **24**, 169-180 (2003).

27 Jian-Tao, Z. *Macro. Mater. Eng.* **294**, 396-404 (2009).

28 Li, X. *J. Col. Int. Sci.* **348**, 408-415 (2010).

29 Monteux, C., Marliere, Paris, P., Pantoustier, N., Sanson, N., Perrin, P. *Langmuir* **26**, 13839-13846 (2010).

30 Romero, S. *Chem. Mater.* **22**, 3051-3059 (2010).

31 Sanson, N. & Rieger, J. *Poly. Chem.* **1**, 965-977 (2010).

32 Wang, B., Guo, Y. & Hu, G. *Mater. Sci. Poland* **28**, 208-215 (2010).

33 Zhou, T. *Polymer* **51**, 3926-3933 (2010).

34 Mallika, D., Sanson, N., Fava, D. *Langmuir* **23**, 196-201 (2007).

35 Nayak, S., Debord, S. & Lyon, A. *Langmuir* **19**, 7374-7379 (2003).

36 Serpe, M., Yarmey, K., Nolan, C., Lyon, A. *Biomacromolecules* **6**, 408-413 (2005).

37 Shivkumar, G. *J. Phys. Chem. B* **114**, 10285-10293 (2010).

38 Snowden, M., Chowdhry, B., Vincent, B., Morris, G. *J. Chem. Soc., Faraday Trans.* **92**, 5013-5016 (1996).

39 Suzuki, D., McGrath, J., Kawaguchi, H., Lyon, A. *J. Phys. Chem. C* **111**, 5667-5672 (2007).

40 Wiedemair, J., Serpe, M., Kim, J., Jongseong, M., Lyon, A., Mizaikoff, B., Kranz, C. *Langmuir* **23**, 130-137 (2007).

41 Sorrell, C. & Lyon, A. *J. Phys. Chem. B* **111**, 4060-4066 (2007).

42 Debord, J. & Lyon, A. *Langmuir* **19**, 7662-7664 (2003).

43 Serpe, M. & Lyon, A. *Chem. Mater.* **16**, 4373-4380 (2004).

44 Jones, C., Serpe, M., Shroeder, L., Lyon, A. *J. Am. Chem. Soc.* **125**, 5292-5293 (2003).

45 Carregal-Romero, S., Buurma, N., Perez-Juste, J., Liz-Marzan, L., Herves, P. *Chem. Mater.* **22**, 3051-3059 (2010).

46 Burmistrova, A. & Klitzing, R. v. *J. Mater. Chem.* **20**, 3502-3507 (2010).

47 Tsuji, S. & Kawaguchi, H. *Langmuir* **21**, 2434-2437 (2005).

48 Nerapusri, V., Keddie, J., Vincent, B., Bushnak, I. *Langmuir* **22**, 5036-5041 (2006).

49 Sakai, T., Takeoka, Y., Seki, T., Yoshida, R. *Langmuir* **23**, 8651-8654 (2007).

50 Meng, Z., Cho, J., Debord, S., Breedveld, V., Lyon, A. *J. Phys. Chem. B* **111** (2007).

51 Julthongpiput, D., Lin, Y., Teng, J., Zubarev, E., Tsukruk, V. *J. Am. Chem. Soc.* **125**, 15912-15921 (2003).

52 Melburne, C., Julthongpiput, D., Bergman, K. *Langmuir* **20**, 10046-10054 (2004).

53 Karg, M., Wellert, M., Prevost, S., *Col. Poly. Sci.*, 1-11 (2010).

54 Delcea, M., Schmidt, S., Palankar, R., Raghavendra, F., Fery, A., Moehwald, H., Skirtach, A. *Small* **6**, 2858-2862 (2010).

55 Schmidt, S., Motschmann, H., Hellweg, T., et al. *Polymer* **49**, 749-756 (2008).

56 Schmidt, S., Hellweg, T. & Klitzing, R. v. *Langmuir* **24**, 12595-12602 (2008).

57 Schmidt, S., Zeiser, M., Hellweg, T., et al. *Adv. Func. Mater.* **20**, 3235-3243 (2010).

58 Diez-Pascual, A. & Wong, J. *J. Col. Int. Sci.* **327**, 79-89 (2010).

59 Jones, C. & Lyon, A. *Langmuir* **19**, 4544 - 4547 (2003).

60 Gan, D. & Lyon, A. *Am. Chem. Soc.* **123**, 7511 - 7517 (2001).

61 Tsukruk, V. & Reneker, D. *Polymer* **36**, 1791-1808 (1995).

62 Tsukruk, V. *Rubber Chem. Tech.* **70**, 430-467 (1997).

63 Tsukruk, V. Ko, H., Peleshanko, S., Phys. Rev. Let. 90, 065502-(1-4) (2004).

64 Callister, W., *Materials Science and Engineering Introduction*. John Willey & Sons, Inc.. 33-40 (2003).

65 Russel, A., Lee, K. *Structure-Property Relations in Nonferrous Metals*. John Willey & Sons, Inc.. 2-4 (2005).

66 Li, D., Lee, J., Kim, D. *J. Coll. Int. Sci.* **354**, 585 - 591 (2011).

67 Zavgorodnya, O., Serpe, M. *Coll. Poly. Sci*. DOI 10.1007/S00396-011-2376-1(2011).

68 Riegler, H. & Essler, F. *Langmuir* **18**, 6694-6698 (2002).